AD-A166 614 PREDICTING HIGH-VOLTAGE CHARGING OF SPACECRAFT IN LOW POLAR ORBIT(U) YORK UNIV DOWNSVIEW (ONTARIO) J G LAFRAMBOISE 30 MAR 85 SCIENTIFIC-1 AFGL-TR-85-0263 F19628-83-K-0028

1/1

UNCLASSIFIED F/G 22/1 NL

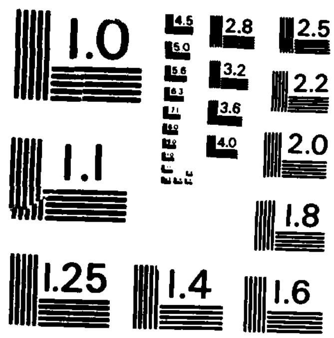

MICROCOPY RESOLUTION TEST CHART
NATIONAL BUREAU OF STANDARDS-1963-A

(12)

AFGL-TR-85-0263

AD-A166 614

PREDICTING HIGH-VOLTAGE CHARGING OF SPACECRAFT
IN LOW POLAR ORBIT

J. G. Laframboise

York University
4700 Keele Street
Downsview, Ontario, Canada M3J 1P3

30 March 1985

Scientific Report No. 1

APPROVED FOR PUBLIC RELEASE; DISTRIBUTION UNLIMITED

AIR FORCE GEOPHYSICS LABORATORY
AIR FORCE SYSTEMS COMMAND
UNITED STATES AIR FORCE
HANSCOM AIR FORCE BASE, MASSACHUSETTS 01731

"This technical report has been reviewed and is approved for publication"

MICHAEL HEINEMANN
Contract Manager
Spacecraft Interactions Branch
Space Physics Division

CHARLES P. PIKE, Chief
Spacecraft Interactions Branch
Space Physics Division

FOR THE COMMANDER

RITA C. SAGALYN, Director
Space Physics Division

This report has been reviewed by the ESD Public Affairs Office (PA) and is releasable to the National Technical Information Service (NTIS).

Qualified requestors may obtain additional copies from the Defense Technical Information Center. All others should apply to the National Technical Information Service.

If your address has changed, or if you wish to be removed from the mailing list, or if the addressee is no longer employed by your organization, please notify AFGL/DAA, Hanscom AFB, MA 01731. This will assist us in maintaining a current mailing list.

Unclassified
SECURITY CLASSIFICATION OF THIS PAGE

AD-A166614

REPORT DOCUMENTATION PAGE

1a. REPORT SECURITY CLASSIFICATION Unclassified	1b. RESTRICTIVE MARKINGS
2a. SECURITY CLASSIFICATION AUTHORITY	3. DISTRIBUTION/AVAILABILITY OF REPORT Approved for public release; Distribution unlimited.
2b. DECLASSIFICATION/DOWNGRADING SCHEDULE	
4. PERFORMING ORGANIZATION REPORT NUMBER(S)	5. MONITORING ORGANIZATION REPORT NUMBER(S) AFGL-TR-85-0263
6a. NAME OF PERFORMING ORGANIZATION York University 6b. OFFICE SYMBOL (If applicable)	7a. NAME OF MONITORING ORGANIZATION Air Force Geophysics Laboratory
6c. ADDRESS (City, State and ZIP Code) 4700 Keele Street Downsview, Ontario, Canada M3J 1P3	7b. ADDRESS (City, State and ZIP Code) Hanscom AFB Massachusetts 01731
8a. NAME OF FUNDING/SPONSORING ORGANIZATION 8b. OFFICE SYMBOL (If applicable)	9. PROCUREMENT INSTRUMENT IDENTIFICATION NUMBER F19628-83-K-0028
8c. ADDRESS (City, State and ZIP Code)	10. SOURCE OF FUNDING NOS.

PROGRAM ELEMENT NO.	PROJECT NO.	TASK NO.	WORK UNIT NO.
62101F	7661	11	AC

11. TITLE (Include Security Classification) Predicting High-Voltage Charging of Spacecraft in Low Polar Orbit

12. PERSONAL AUTHOR(S)
J. G. Laframboise

13a. TYPE OF REPORT	13b. TIME COVERED	14. DATE OF REPORT (Yr., Mo., Day)	15. PAGE COUNT
Scientific Report #1	FROM ______ TO ______	1985 March 30	46

16. SUPPLEMENTARY NOTATION

17. COSATI CODES			18. SUBJECT TERMS (Continue on reverse if necessary and identify by block number)
FIELD	GROUP	SUB. GR.	Spacecraft charging, Low polar orbit, Auroral Ionosphere, Electron escape, Computer code

19. ABSTRACT (Continue on reverse if necessary and identify by block number)

The work presented in this report is in two parts. In the first, we develop a simple approximate prediction of the required conditions for high-voltage polar-orbit charging. The results suggest that for any given spacecraft, surface potentials are likely to depend more strongly on the ratio of ambient flux of high-energy electrons to that of all ions, than on any other environmental parameter. In the second part of this report, we present results of a numerical calculation of secondary-electron escape currents from negatively-charged spacecraft surfaces having various orientations relative to the local magnetic-field direction.

20. DISTRIBUTION/AVAILABILITY OF ABSTRACT UNCLASSIFIED/UNLIMITED ☐ SAME AS RPT. ☒ DTIC USERS ☐	21. ABSTRACT SECURITY CLASSIFICATION Unclassified

22a. NAME OF RESPONSIBLE INDIVIDUAL	22b. TELEPHONE NUMBER (Include Area Code)	22c. OFFICE SYMBOL
Michael Heinemann		AFGL/PHK

DD FORM 1473, 83 APR EDITION OF 1 JAN 73 IS OBSOLETE.

Unclassified
SECURITY CLASSIFICATION OF THIS PAGE

TABLE OF CONTENTS

1. INTRODUCTION

High-voltage charging is now recognized (Parks and Katz, 1981; Katz and Parks, 1983) to be an operating hazard for larger spacecraft, including the Shuttle orbiter, passing through the auroral plasma in low polar orbit. It is important to develop methods for predicting which combinations of environmental conditions and spacecraft properties will result in high-voltage charging.

The work presented in this Report is in two parts. Section 2 contains a simple approximate theoretical prediction of the required conditions for high-voltage polar-orbit charging. The results of this derivation suggest that spacecraft potentials are likely to depend more strongly on the ratio of ambient flux of high-energy electrons to that of all ions, than on any other environmental parameter. In Sec. 3, calculations are made of secondary-electron escape currents from spacecraft surfaces, as influenced by magnetic fields having various directions relative to these surfaces. For realistic values of electron-repelling surface electric fields, the results show an extreme sensitivity of escaping currents to small changes in surface orientation, for surfaces almost parallel to the magnetic field direction. This implies that the occurrence of high-voltage charging in marginal circumstances may depend very strongly on the precise orientation of a surface. Appendix A contains a listing of the computer program used to perform these calculations.

2. ESTIMATE OF REQUIRED ENVIRONMENTAL CONDITIONS FOR LOW-POLAR-ORBIT CHARGING

In this Section, we show that spacecraft surface potentials are likely to depend more strongly on the ratio of ambient flux of high-energy electrons to that of all ions than on any other applicable environmental parameter. To do this, we make the following approximations.

(1) We assume that magnetic-field effects on charged-particle motion are negligible. This assumption should be acceptable for initial estimates because the gyroradii of ions and high-energy electrons are generally a few metres or larger, especially in a high-voltage sheath (Laframboise, 1983, Table 1), and collection of "cold" (~0.1 eV) ionospheric electrons by a negatively-charged spacecraft will be very small, so their density is well-approximated by a Boltzmann factor, independently of the presence of a magnetic field.

(2) We assume that ambient high-energy electrons have an isotropic velocity distribution. Large departures from this have been observed in auroral-plasma conditions (W.J. Burke, 1984, private communication), but this should not seriously affect the type of rough estimate made here. Parks and Katz, 1981, and Katz and Parks, 1983, assumed both the ion and electron fluxes to be unidirectional; we discuss this point later in this Section.

(3) We ignore secondary-electron emission; magnetic-field effects would tend to suppress this on some parts of the spacecraft in any case (J.G. Laframboise, 1983, 1985; Sec. 3).

(4) We assume that the spacecraft is a unipotential sphere, large compared to the typical ambient Debye length of $\lesssim$ 1 cm. We consider only <u>overall</u> charging of the spacecraft. This neglects the possibility that <u>local</u> high-voltage charging may occur, especially on surfaces in the spacecraft wake.

(5) We assume that both ions and electrons have double-Maxwellian velocity distributions, with the colder component in either case having a temperature of 0.1 eV, and the hotter 1 keV or larger. In the spacecraft reference frame, these are superposed on a drift velocity equal and opposite to the spacecraft velocity.

(6) Ions are assumed to be either H^+ or O^+.

Note that assumption (3) could cause a false prediction that high-voltage charging occurs, while assumption (4) could cause a false prediction that it does not. The effects of assumptions (1), (2), and (5) are less clear; these could conceivably either increase or decrease predicted surface potentials. With regard to (6), assuming that the ions are H^+ results in maximum wake-filling by ions. If there are any electrically-isolated surfaces in the spacecraft wake, this would result

in decreased surface potentials (magnitudes); assuming O^+ gives the reverse.

Probably the most serious difficulty in formulating a theory for low-orbit-charging is the prediction of ion collection on downstream surfaces. As mentioned in assumption (3) above, we avoid this difficulty by considering only total, rather than local, ion collection, on a unipotential sphere. Kanal [1962, Eq. (63)] gives an expression for the ion current collected by such a sphere from a drifting Maxwellian plasma in the limit of zero potentials (relative to space potential), as follows:

$$i_i = \tfrac{1}{2} \left[\pi^{\frac{1}{2}} \left(S_i + \frac{1}{2S_i}\right) \operatorname{erf}(S_i) + \exp(-S_i^2)\right] \tag{2.1}$$

where $i_i = I_i/I_{oi}$, I_{oi} is the ion random current $en_{i\infty}(kT_i/2\pi m_i)^{\frac{1}{2}}$, $S_i = U/(2kT_i/m_i)^{\frac{1}{2}}$ is the ion speed ratio, U is the ion drift speed relative to the spacecraft, e is the magnitude of the electronic charge, k is Boltzmann's constant, and m_i, T_i, and $n_{i\infty}$ are ion mass, temperature, and ambient number density. We assume that U = 8 km/sec, corresponding to low circular orbit.

We need to take account of the effect of a large ion-attracting surface potential on ion collection, in the limit of small Debye length λ_D compared to the sphere radius r_s. To do this, we use a result of Parrot et al (1982). These authors show that for a probe in a collisionless, nonmagnetized, Maxwellian plasma having $T_i/T_e = 1$ and <u>without</u>

ion drift, and in the limit when $\lambda_D/r_s \rightarrow 0$ but $-e\phi_s/kT >> 1$ [where these limits must be approached in such a way that $(-e\phi_s/kT)(\lambda_D/r_s)^{4/3}$ remains << 1, i.e. sheath thickness remains << sphere radius], the ion (attracted-particle) current is larger than the random current by a factor of 1.45. This factor represents the effect of the "presheath" potential on ion collection. Even though several of their assumptions are unfulfilled in our case, the resulting effects on ion collection are probably small enough for our purposes. We therefore multiply Eq. (2.1) by the same factor to obtain an estimate of total ion collection as influenced by surface-potential effects. The resulting ion-current dependence on ion speed ratio is plotted in Fig. 2.1. For O^+ ions at T = 0.1 eV (1160K), H^+ at 0.1 eV, O^+ at 1 keV, and H^+ at 1 keV, S_i = 7.31, 1.83, 0.0731, and 0.0183 (the latter two are effectively zero), respectively. The corresponding ion-current enhancement factors (values of i_i) from Fig. 2.1 are 9.50, 2.69, 1.45, and 1.45, respectively.

If the ambient ions are H^+, the ion collected current is now given by:

$$\begin{aligned} I_i &= 4\pi r_s^2 \, e n_{ic} \left\{ \frac{kT_{ic}}{2\pi m_i} \right\}^{\frac{1}{2}} (2.69) \\ &+ 4\pi r_s^2 \, e n_{ih} \left\{ \frac{kT_{ih}}{2\pi m_i} \right\}^{\frac{1}{2}} (1.45) \end{aligned} \qquad (2.2)$$

where the subscripts ic and ih refer to the cold and hot ion populations. If the ions are O^+, then the factor 2.69 in (2.2) should be replaced by 9.50.

The electron collected current is:

$$I_e = 4\pi r_s^2 e n_{ec} \left\{ \frac{kT_{ec}}{2\pi m_e} \right\}^{\frac{1}{2}} \exp \left\{ \frac{e\phi_s}{kT_{ec}} \right\}$$

$$- 4\pi r_s^2 e n_{eh} \left\{ \frac{kT_{eh}}{2\pi m_e} \right\}^{\frac{1}{2}} \exp \left\{ \frac{e\phi_s}{kT_{eh}} \right\} . \qquad (2.3)$$

If high-voltage charging occurs, then $-e\phi_s >> kT_{ec}$, and the first term on the right-hand side of this equation becomes negligible.

For current balance, $I_i = I_e$. This leads to:

$$2.69 n_{ic} \sqrt{T_{ic}} + 1.45 n_{ih} \sqrt{T_{ih}} = n_{eh} \sqrt{m_i/m_e} \sqrt{T_{eh}}\, e^{-e|\phi_s|/kT_{eh}} \qquad (2.4)$$

where $\sqrt{m_i/m_e} = 43$ for H^+ ions. Therefore:

$$e|\phi_s|/kT_{eh} = \ln \left[\frac{43 n_{eh} \sqrt{T_{eh}}}{2.69 n_{ic} \sqrt{T_{ic}} + 1.45 n_{ih} \sqrt{T_{ih}}} \right] \qquad (2.5)$$

for H^+ ions, with 43 and 2.69 replaced by 172 and 9.50 for O^+ ions. This is equivalent to:

$$e|\phi_s|/kT_{eh} = \ln \left[\frac{\text{hot-electron ambient flux}}{2.69\ (\text{cold-ion ambient flux}) + 1.45\ (\text{hot ion ambient flux})} \right] \qquad (2.6)$$

For high-voltage charging to become probable, the argument of the $\ln$ function must be close to or larger than e $\simeq$ 2.72, i.e:

$$\frac{\text{hot-electron ambient flux}}{2.59\,(\text{cold-ion ambient flux}) + 1.45(\text{hot-ion ambient flux})} \gtrsim 2.72. \tag{2.7}$$

For O^+/H^+ mixtures and for hot-ion temperatures other than 1 keV, generalization of this result is straightforward. Since any hot ions are likely to have $T_{ih}/T_{ic} \simeq 10^4$, the hot-ion ambient flux will exceed the cold-ion ambient flux if the hot ions constitute more than about 1% of the total ambient-ion number density. Equation (2.7) indicates that the onset of high-voltage charging can be expected to depend primarily on the ratio of hot-electron ambient flux to the ambient flux of <u>all</u> ions, as mentioned at the beginning of this Section. This completes our argument in support of this conclusion.

In analyzing spacecraft data, one is therefore likely to find better correlation of spacecraft voltages with the ratio which appears in Eq. (2.7) (or something nearly equal to it) than with any other measurable quantity, such as electron or ion density or average energy, taken individually. In calculating values of this ratio, the ambient fluxes which are involved need to have been measured <u>simultaneously</u> on the same spacecraft. Even though the approximations made in deriving (2.7) are severe, and the precise dependence of spacecraft voltages on this ratio may therefore differ substantially from that given in Eq. (2.7) (and/or the coefficients in the ratio itself may need to be modified), our

general conclusion, i.e. that spacecraft voltages should correlate most strongly with this ratio (or something nearly equal to it), is likely to remain valid. Furthermore, the dependence of spacecraft voltages on this flux ratio is likely to retain an approximately exponential form. In situations where most secondary and backscattered electrons emitted by the spacecraft will escape (see Sec. 3), primary-electron incident fluxes will be approximately cancelled for many spacecraft materials by electron escape at incident energies up to a few keV (Laframboise et al, 1982; Laframboise and Kamitsuma, 1983), so the hot-electron ambient flux term in (2.7) needs to be modified accordingly.

The most serious approximation made in deriving (2.7) is probably item (4) in the list at the beginning of this Section. This is because ion fluxes on downstream surfaces are likely to be very much smaller than their average over the entire spacecraft. They are also likely to be strongly dependent on spacecraft geometry, local surface potential distribution, and O^{+}/H^{+} concentration ratio. Therefore, the critical value of ambient flux ratio, at which the onset of high-voltage charging occurs, is likely to vary substantially among spacecraft having different geometries and surface materials. In particular, for spacecraft having electrically-isolated downstream surfaces, this critical ratio is likely, because of local charging on these surfaces, to be much lower than for spacecraft which have an entirely conductive surface.

Furthermore, in contrast with the situation for total ion collection,

there is no known, simple, reliable method for estimating ion fluxes on downstream surfaces. Parks and Katz (1983a,b) have developed an ion flux calculation for the downstream point on a sphere in a potential which has a given, simple analytic form. Detailed numerical simulation, which includes realistic self-consistent spacecraft sheath potential distributions, and which probably needs to involve at least some ion orbit-following, therefore appears to be essential. Preliminary indications, from work of this type presently in progress (L.W. Parker and J.G. Laframboise, to be published), are that conditions on the "shoulder" or "side-point" regions of spacecraft (surface material and geometry of this region; local surface curvature is probably important) may strongly influence potentials of downstream surfaces, because of detailed effects on ion trajectories. The geometry being investigated first is an infinite nonconducting cylinder transverse to the ion drift direction; and preliminary results also indicate that the location of maximum negative surface voltage is not at the downstream point but at two points symmetrically located on either side of it.

So far, we have not mentioned the difficulties which can arise in measuring the ambient ion fluxes which appear in Eq. (2.7). So far, we have also defined "ambient flux" to be that measured in an Earth-fixed reference frame. The alternative would be to define it as that measured in the spacecraft frame, i.e. including ram effects. Ion fluxes measured by spacecraft instruments are strongly influenced by ram effects. In fact, the numerical factors 2.69, 1.45, and 9.50, which

appear in Eq. (2.7) and the associated discussion, already constitute a rough ram-effect correction, but for total current to a sphere, not for local collection by a forward-facing instrument aperture. It may happen that the ram-effect correction factors for an instrument are nearly equal to the above factors, so that the instrument measurement, without any correction, already gives a good estimate of the denominator of Eq. (2.7). In any case, the response of the instrument will depend on its geometry, and this problem has already been treated by other authors (Parker, 1970; Parker and Whipple, 1970; Whipple et al, 1974; Chang et al, 1979; Singh and Baugher, 1981; Comfort et al, 1982; Laframboise, 1983), so we do not discuss it here.

Parks and Katz (1981) and Katz and Parks (1983) have estimated charging potentials on spherical spacecraft of 0.5m and 5m radius, assuming that the ions are O^+, the hot electron temperature T_{eh} is 5 keV, and spacecraft speed is 8 km/sec. Their results can be compared directly with those given by our Eqs. (2.5) - (2.7). They have used the theory of Langmuir and Blodgett (1924) to obtain values for sheath radius as a function of spacecraft potential. They present spacecraft potentials as functions of the ratio κ of hot ("precipitating") electron ram current to ion ram current. To make a comparison, their value of κ needs to be expressed in terms of our ambient flux ratio. They have assumed the ambient electron flux to be unidirectional. To convert to an equivalent isotropic flux, we note that current to a sphere = $4\pi r_s^2 \times$ isotropic (random) flux, but = $\pi r_s^2 \times$ unidirectional (ram) flux.

Therefore, equivalent isotropic flux = $\frac{1}{4}$ × unidirectional flux, for a sphere.

Also for a sphere, the ratio of ion ram to random currents is $U/(8\kappa T_i/\pi m_i)^{\frac{1}{2}} = \frac{1}{2}\sqrt{\pi}\, S_i$. Using $S_i = 7.31$, this ratio = 6.48, so therefore:

$$
\begin{aligned}
\text{their } \kappa &= \frac{\text{hot electron ram current}}{6.48 \times \text{total ion random current}} \\
&= \frac{\pi r_s^2 \times \text{hot electron ram flux}}{6.48 \times 4\pi r_s^2 \times \text{total ion random flux}} \\
&= \frac{1}{6.48} \times \frac{\text{hot electron (equivalent) random flux}}{\text{total ion random flux}} \\
&= \frac{1}{6.48} \times \text{our flux ratio R.}
\end{aligned}
\tag{2.8}
$$

With coefficients for O^+ used, our Eq. (2.6) gives:

$$\phi_s = -5000 \ln (R/9.50). \tag{2.9}$$

Figure 2.2 shows our result and theirs [from their Fig. 3 (1981) or Fig. 2 (1983)], plotted together. At larger potentials, the combined set of results shows a monotonic progression toward increased charging for larger spacecraft. For $-\phi_s < 350$V, their 5m sphere shows more charging than our large-radius-limit sphere. This is because their ion-current enhancement factor, which is determined by the size of a sharp-edged Langmuir-Blodgett sheath, falls below ours, which includes the effect of a quasineutral presheath. This discussion suggests that the

tendency toward high-voltage charging always increases with spacecraft size, but magnetic-field effects may modify this (Laframboise, 1983, Sec. 1). The corresponding curves for local charging, on surfaces in a spacecraft wake, will lie to the left of those shown in Fig. 2.2, but these remain to be computed numerically.

3. CALCULATION OF SECONDARY-ELECTRON ESCAPE CURRENTS FROM NEGATIVELY-CHARGED SPACECRAFT SURFACES IN A MAGNETIC FIELD

3.1 SUMMARY

In low Earth orbit, the geomagnetic field $\vec{B}$ is strong enough that secondary electrons emitted from spacecraft surfaces have an average gyroradius much smaller than typical dimensions of large spacecraft. This implies that escape of secondaries will be strongly inhibited on surfaces which are nearly parallel to $\vec{B}$, even if a repelling electric field exists outside them. This effect is likely to make an important contribution to the current balance and hence the equilibrium potential of such surfaces, making high-voltage charging of them more likely. We present numerically-calculated escaping secondary-electron fluxes for these conditions. For use in numerical spacecraft-charging simulations, we also present an analytic curve-fit to these results, accurate to within 3% of the emitted current.

3.2 INTRODUCTION

The prediction of high-voltage charging or other environmental effects on a spacecraft in low Earth orbit appears likely to be more complicated than in geostationary orbit, for at least three reasons.

These reasons are: (a) space-charge effects (on sheath and wake potentials) are more important, because space-charge densities are much higher (the Debye length is no longer >> typical spacecraft dimensions) (b) ion flow

effects are more important, because spacecraft orbital speed $\tilde{>}$ ion thermal speeds (c) the geomagnetic field $\vec{B}$ is likely to have an important influence on charged-particle motions because $\vec{B}$ is now much larger, and not all of the average particle gyroradii of importance are any longer >> typical spacecraft dimensions.

We wish to investigate an important consequence of (c), which concerns the escape of secondary electrons emitted from spacecraft surfaces. Our discussion will also apply, with minor modifications, to photoelectron or backscattered-electron escape. In low Earth orbit, in the auroral-zone geomagnetic field ($|\vec{B}| = 0.44$ gauss $= 4.4 \times 10^{-5}$ T), the gyroradius of a "typical" 3eV secondary electron and a 10 keV auroral electron are 13 cm and 8 m, respectively. The average gyroradius of "cold" ionospheric electrons (temperature $T = 0.1$ eV) in the same $\vec{B}$ is even smaller (2 cm), but this is not an important parameter in most cases because these electrons are repelled if the spacecraft potential is negative, and their density is then well-approximated by a Boltzmann factor, which is unaltered by $\vec{B}$ effects.

The reason why $\vec{B}$ affects secondary-electron escape is shown in Fig. 3.1. In Fig. 3.1(a), the spacecraft surface is perpendicular to $\vec{B}$, and the emitted electrons, which experience an electric force $-e\vec{E}$ directed away from the surface, all escape, helping to discharge it. In Fig. 3.1(b), the spacecraft surface is nearly parallel to $\vec{B}$, and almost all of the emitted electrons return to it, even though they still experience an electric force directed away from it. These electrons therefore are unable to help discharge it, so a surface nearly parallel to $\vec{B}$ is more likely to charge to a large negative voltage. Note that the component of $\vec{E}$ which is perpendicular to $\vec{B}$ results only in an $\vec{E} \times \vec{B}$ drift

parallel to the surface.

For any object much larger than 13 cm, the escape of secondary electrons will be strongly affected by this process. For example, most surfaces on the Shuttle are effectively "infinite planes" by this criterion. On the other hand, the average gyroradius of high-energy auroral electrons is comparable to Shuttle dimensions, so the deposition of these electrons onto Shuttle surfaces is likely to be only moderately inhibited.

For a larger object (size >> 8 m), deposition of auroral electrons will also become strongly orientation-dependent, with both collection and escape of electrons now being inhibited on surfaces nearly parallel to $\vec{B}$. This suggests that high-voltage charging of such surfaces may be more likely on objects of intermediate size than on either larger or smaller ones. In the calculation of Parks and Katz (1981), Katz and Parks (1983), the tendency toward high-voltage charging increased with spacecraft size because in their model, ion collection increased less rapidly with spacecraft size than did electron collection. To determine which of these two effects predomiates will require more detailed calculations than have been done so far.

As already mentioned, strong ion flow effects also are generally present in low orbit; the ion speed ratios (flow speed/most probable ion thermal speed) for H^+ at 1 keV, H^+ at 0.1 eV, and O^+ at 0.1 eV are 0.02, 1.8, and 7.3, respectively. Whenever the latter is the predominant ion species, ion

collection on downstream surfaces will therefore be strongly inhibited. If a surface is simultaneously downstream and nearly parallel to $\vec{B}$, as is likely to be the case in the auroral zones, then the tendency for high-voltage charging to occur on it will be greatly increased (Fig. 3.2).

To "straightforwardly" include $\vec{B}$ effects on secondary-electron emission in a large two or three dimensional simulation program would involve the numerical integration of very large numbers of secondary-electron orbits. The resulting computing costs usually would be formidable, especially since these orbits would have relatively large curvatures. A desirable alternative is to "parameterize" the situation by treating in advance a simplified but still sufficiently realistic model problem. In order to do this, we make the approximations described in Sec. 3.3.

3.3 THEORY FOR $\vec{E}$ NORMAL TO SURFACE

We assume that the spacecraft surface is an infinite plane, and the electric and magnetic fields $\vec{E}$ and $\vec{B}$ outside it are uniform. In the work presented here, we also assume that the electric force $-e\vec{E}$ on electrons is directed along the outward normal to the surface; here e is the magnitude of the elementary charge. This assumption is to be relaxed later (J.G. Laframboise, to be published) in order to permit variations of potential along the surface to be taken into account. We assume that the secondary electrons are emitted with a Maxwellian distribution corresponding to a temperature T. The ratio $i=I/I_0$ of escaping to emitted flux is then a function of two parameters: the angle θ between the surface normal and the direction of $\vec{B}$ (Fig. 3.3), and a parameter

describing the strength of E. A convenient choice for this parameter is the difference in potential across a mean secondary-electron gyroradius $a = (1/eB)(\pi mkT/2)^{\frac{1}{2}}$, divided by kT/e, where m is electron mass and k is Boltzmann's constant.

This quotient is:

$$\epsilon \equiv \frac{E}{B} \sqrt{\frac{\pi m}{2kT}} \tag{3.1}$$

where $E \equiv |\vec{E}|$ and $B \equiv |\vec{B}|$.

This quantity also has an alternative, more useful interpretation: it is the ratio of the magnitude $|\vec{E} \times \vec{B}|/B^2$ of the $\vec{E} \times \vec{B}$ drift speed, to one-half the mean thermal speed $(8kT/\pi m)^{\frac{1}{2}}$ of the emitted electrons. It is useful to estimate the value of ϵ for a high-voltage spacecraft sheath in low-orbit conditions. To do this, we use the sheath solution of Al'pert et al (1965, Table XXIV and Fig. 72). For a 1 kV and a 5 kV sheath around a sphere of radius 3m in a collisionless plasma having an ambient ion temperature of 0.1V, number density of $3 \times 10^5\ cm^{-3}$, and resultant (ion) Debye length of 0.43 cm, their results give, respectively, sheath thicknesses of 2.6 and 6.1 m, and surface electric fields E = 0.86 and 2.9 kV/m. Using $B = 4.4 \times 10^{-5}$ T and T = 3 eV for secondary electrons, we then obtain ϵ = 33.9 and 114.2. Both of these are relatively large values, whose significance can be understood if we consider what would happen if ϵ were infinite.

In this limit, it is easy to show that secondary electrons would all escape unless $\vec{B}$ were exactly parallel to the surface (θ were 90°). This can be shown as follows. In this limit, secondary electrons would have no "thermal" motion. The (y,z) projection of their motion would then be similar to that shown in Fig.3.4 . This motion would be the sum of: (i) an $\vec{E} \times \vec{B}$ drift in the y direction (ii) a uniform acceleration along $\vec{B}$, whose projection in the (y,z) plane would be upward (iii) just enough gyromotion to produce a cycloidal path when combined with (i), so that in the absence of (ii), the electron would (just) return to the surface at the end of each gyroperiod. In the presence of (ii), these "return points" are displaced upward by progressively increasing amounts (Fig.3.4), so the electron can never return to the surface, unless $\vec{B}$ is exactly parallel to the surface, so that the upward component of $-e\vec{E}$ along $\vec{B}$ vanishes. If $-e\vec{E}$ has a component parallel to the surface, this conclusion needs to be modified (J.G. Laframboise, to be published).

This result suggests that for large finite values of ϵ (including the values calculated above), electron escape is likely to be almost complete except for θ very near 90°, where it should drop to zero very steeply. The occurrence of high-voltage charging in marginal circumstances may therefore depend very strongly on the precise orientation of a surface.

The escaping secondary-electron flux is given by:

$$I = \iiint f(\vec{v}_o)\, H(\vec{v}_o)\, v_{oz}\, d^3 \vec{v}_o$$

$$= \int_{-\infty}^{\infty} dv_{ox} \int_{-\infty}^{\infty} dv_{oy} \int_{0}^{\infty} n \left\{ \frac{m}{2\pi kT} \right\}^{3/2} \exp\left\{ - \frac{mv_o^2}{2kT} \right\} H(v_{ox}, v_{oy}, v_{oz}) v_{oz} dv_{oz}$$

(3.2)

where: $\vec{v}_o$ is the initial velocity of an emitted electron, $f(\vec{v}_o) \equiv d^3n/d^3\vec{v}_o$ is the velocity distribution of emitted electrons, n is a reference number density, and $H(\vec{v}_o)$ is equal to 1 for escaping electrons and 0 for those which return to the surface. The emitted flux is:

$$I_o = n(kT/2\pi m)^{\frac{1}{2}}. \tag{3.3}$$

We also introduce the dimensionless velocity:

$$\vec{u} = \vec{v}\,(m/2kT)^{\frac{1}{2}}. \tag{3.4}$$

Equation (3.2) then becomes:

$$\frac{I}{I_o} = \frac{2}{\pi} \int_{-\infty}^{\infty} \int_{-\infty}^{\infty} du_{ox} du_{oy}\, e^{-u_{ox}^2 - u_{oy}^2} \int_{0}^{\infty} du_{oz} u_{oz}\, e^{-u_{oz}^2} H(u_{ox}, u_{oy}, u_{oz})$$

$$= \frac{1}{\pi} \int_{-\infty}^{\infty} \int_{-\infty}^{\infty} du_{ox} du_{oy} \exp(-u_{ox}^2 - u_{oy}^2) \sum_{k=1}^{k_{max}(u_{ox}, u_{oy})} (-1)^{k+1} \times \exp[-u_{lim,k}^2(u_{ox}, u_{oy})]$$

$$\approx \frac{1}{\pi} \sum_i \sum_j \Delta u_{ox} \Delta u_{oy} \exp(-u_{ox,i}^2 - u_{oy,j}^2) \sum_{k=1}^{(k_{max})_{i,j}} (-1)^{k+1} \times \exp[(-u_{lim,k}^2)_{i,j}] \tag{3.5}$$

which is in a form suitable for numerical summation. The quantities $u_{lim,1}$,

$u_{lim,2}, \dots, u_{lim,k_{max}}$ are the values of u_{oz} for which H changes between 0 and 1 for each u_{ox} and u_{oy}. These values must be found by numerically determining which particle orbits reimpact the surface. These orbits can, however, be determined in analytic form, with time as a parameter. To do this, we use the coordinate system shown in Fig. 3.3, together with a y-axis (not shown) directed into the plane of the Figure. The equation of motion for an electron is:

$$\dot{\vec{v}} = -\frac{e}{m}(\vec{E} - \vec{v} \times \vec{B}). \tag{3.6}$$

We solve this with the initial conditions $\xi = y = \eta = 0$, $v_\xi = v_{o\xi}$, $v_y = v_{oy}$, and $v_\eta = v_{o\eta}$. We introduce the dimensionless variables:

$$\epsilon_x = \frac{E_x}{B}\sqrt{\frac{\pi m}{2kT}}, \quad \epsilon_y = \frac{E_y}{B}\sqrt{\frac{\pi m}{2kT}}, \quad \text{etc};$$

$$\tilde{x} = x/\bar{a}, \ \tilde{y} = y/\bar{a}, \ \text{etc}; \tag{3.7}$$

$$\tau = \omega_c t = (eB/m)t.$$

In the present work, ϵ_x and ϵ_y are both zero, but for future use, we have retained these quantities in the formulas below. We obtain:

$$u_{o\xi} = u_{ox} \sin\theta + u_{oz} \cos\theta;$$

$$u_{o\eta} = -u_{ox} \cos\theta + u_{oz} \sin\theta;$$

$$\tilde{\xi} = \frac{-1}{\pi}\epsilon_\xi \tau^2 + \frac{2}{\sqrt{\pi}} u_{o\xi}\, \tau;$$

$$\tilde{y} = \left\{\frac{2}{\sqrt{\pi}} u_{oy} - \frac{2}{\pi}\epsilon_\eta\right\} \sin\tau + \left\{\frac{2}{\sqrt{\pi}} u_{o\xi} + \frac{2}{\pi}\epsilon_y\right\} (\cos\tau - 1) + \frac{2}{\pi}\epsilon_\eta \tau;$$

$$\tilde{\eta} = \left\{\frac{2}{\sqrt{\pi}} u_{o\eta} + \frac{2}{\pi}\epsilon_y\right\} \sin\tau + \left\{\frac{2}{\sqrt{\pi}} u_{oy} - \frac{2}{\pi}\epsilon_\eta\right\} (1-\cos\tau) - \frac{2}{\pi}\epsilon_y \tau; \qquad (3.8)$$

$$\tilde{z} = \tilde{\xi} \cos\theta + \tilde{\eta} \sin\theta.$$

Equations (3.8) can also be differentiated to find $d\tilde{z}/d\tau$. The numerical procedure for finding the quantities $u_{lim,k}$ in Eq. (3.5) then involves calculating $\tilde{z}$ and $d\tilde{z}/d\tau$ at a succession of points along an orbit (if $-e\vec{E}$ is normal to the surface, the electron will reimpact during the first gyroperiod $0 < \tau \le 2\pi$ if at all, so this interval always suffices), and making the appropriate tests on these quantities to find out whether the orbit reimpacts or escapes. For each $u_{ox,i}$ and $u_{oy,j}$ this is done for a succession of values of u_{oz}. These tests also yield the local minimum of $\tilde{z}(\tau)$ if one exists. Whenever a change occurs between no escape and escape from one such value of u_{oz} to the next, an interpolation using these minima can be used to provide the corresponding value of $u_{lim,k}$. In cases where they are unavailable, the arithmetic mean of the two successive u_{oz} values is used.

This completes the definition of the procedure used for calculating the ratio I/I_o of escaping to emitted flux.

3.4 RESULTS AND DISCUSSION

Escaping secondary-electron current densities, computed as described in Sec. 3.3, are shown in Table 1 and Fig. 3.5. Each value of $i = I_o$ was calculated using 191808 orbits, evenly spaced in the intervals $-4.5 \le u_{ox} \le 4.5$, $-4.5 \le u_{oy} \le 4.5$, and $0 \le u_{oz} \le 4.5$, with points on the orbits calculated at intervals $\Delta\tau = \pi/45$. For 8 values each of ϵ and θ, the resulting calculation took 83 hr total on a Hewlett-Packard 1000F minicomputer with Vector Instruction Set. The results are accurate to within about 0.5% or better. The result for $\epsilon = 0$ is just the analytic result $i = \cos\theta$. To see why this is so, we consider the electron orbit shown in Fig. 3.6, which has been fictitiously extended so as to pass through the surface and re-emerge from it. In the absence of an electric field ($\epsilon = 0$), this orbit has the same speed at the re-emergence point C as at the emission point A. Since we have also assumed that the emitted velocity distribution is isotropic, and therefore a function of speed only, the real orbit, for which C is the emission point, must carry the same population as would the fictitious re-emerged orbit. The flux crossing the reference surface DE, which is $\perp \vec{B}$, is therefore the same as if such passages and re-emergences actually occurred, and is the same as if another reference surface FG, also $\perp \vec{B}$, were emitting electrons having the same velocity distribution. However, in reality, the electrons come from the real surface HJ, which is not $\perp \vec{B}$, and all the electron-orbit guiding centers which are inside any given magnetic-flux tube through DE will also be inside the

projection of the same flux tube onto HJ, and the ratio of the intersection areas of this tube with HJ and DE is just sec θ. The ratio of escaping to emitted flux must therefore be the reciprocal of this, or cos θ, as stated above.

Also evident in Fig. 3.5 is the fact, mentioned in Sec. 3.3, that when ϵ is large enough, electron escape becomes essentially complete except when θ is very nearly 90^0. In a real situation, $\vec{E}$ would not be uniform, but would decrease with distance from the surface, contrary to our assumptions. Our results can therefore be expected to overestimate electron escape. This would probably not be a large effect, but this presumption remains to be verified. An approximate compensation for it can be made by calculating ϵ using an electric field value which is averaged over the first mean gyroradius distance from the surface.

The results in Table 1 are approximated to within 2.5% of I_o by the empirical formula:

$$a = 1 + 1.35\epsilon^{1.1394} \exp\left\{0.083725 \left\{1+\tanh\left[1.9732 \ln\left(\frac{\epsilon}{1.13}\right)\right]\right\} -0.07825 \ln\left[1 + (\epsilon/8.5)^{1.78148}\right]\right\};$$

$$b = 0.38033\epsilon^{0.95892} \exp\left\{2.0988\left\{1 + \tanh\left[1.49 \ln\left(\frac{\epsilon}{3.26}\right)\right]\right\}\right\};$$

$$c = \ln(90^o/\theta); \qquad (3.9)$$

$$i = \cos\left[90^o \exp(-ac-bc^2)\right].$$

This formula also has the correct limiting behavior when $\epsilon \to 0$ or ∞, or $\theta \to 0^0$

or 90°. An approximation formula for the emitted flux is also available [Eqs. (5) and (6) of Laframboise et al (1982), and Laframboise and Kamitsuma (1983).

3. 5. CALCULATION OF SECONDARY-ELECTRON DENSITIES

Once the secondary-electron escape fluxes are known (Sec. 3.4), a simple, inexpensive, approximate calculation of their space-charge density distribution can be set up. The proposed method is as follows: (1) ignore the gyromotion of the secondary electrons once they have escaped. Their motion then involves: (a) an acceleration along magnetic field lines, of amount $-(e/m)\vec{E}\bullet\vec{B}/B$ (b) a drift motion of velocity $\vec{E} \times \vec{B}/B^2$ across magnetic field lines. (2) Integrate enough of the trajectories defined by this motion (i.e. their guiding-center trajectories) to define trajectory tubes whose cross-section at any point can be calculated with sufficient accuracy; the method described by Laframboise et al (1982, Sec. 7), can be used to calculate the area of a trajectory tube without reference to neighbouring trajectories. (3) Calculate their space-charge density $n(\vec{r})$ at any point by (a) ignoring the "thermal" spread of their velocities (b) then invoking the fact that their density × their velocity [as given by the orbit integration mentioned in (2)], × the cross-sectional area $A(\vec{r})$ of the trajectory tube (which must be calculated in a plane ⊥ the trajectory) at the point $\vec{r}$ in question, = a constant (whose value is given by the initial conditions at the point on the spacecraft where the trajectory originates) (c) finding their velocity at the point in question by using energy conservation, together with the values of electric potential $\phi(\vec{r})$ and ϕ_o at that point and the emission point, and their assumed velocity v_o at the emission point. The

result is:

$$n(\vec{r}) = n_o v_o A_o / \left\{ A(\vec{r}) \sqrt{v_o{}^2 + (2e/m)\,[\phi(\vec{r}\,) - \phi_o]} \right\} \tag{3.10}$$

where $n_0 v_0$ is the escaping flux calculated in Sec. 3.4. At most positions, $n(\vec{r})$ will be insensitive to the precise value assumed for $v_0{}^2$; assuming that v_0 = the one-sided thermal speed $(2kT/\pi m)^{\frac{1}{2}}$ will suffice for most purposes.

REFERENCES

Al'pert, Ya.L., Gurevich, A.V., and Pitaevskii, L.P. (1965) Space Physics with Artificial Satellites, Consultants Bureau, New York.

Chang, J-S., Godard, R., and Laframboise, J.G. (1979), Mass-discrimination in ion and neutral extraction by mass-spectrometers under spacecraft conditions, Planet. Space Sci. 27, 1213-1220.

Comfort, R.H., Baugher, C.R., and Chappell, C.R. (1982), Use of the thin sheath approximation for obtaining ion temperatures from the ISEE 1 limited aperture RPA, J. Geophys. Res. 87 (A7), 5109-5123.

Kanal, M. (1962) Theory of current collection of moving spherical probes. Space Physics Research Lab., University of Michigan, Ann Arbor, report JS-5.

Katz, I., and Parks, D.E. (1983) Space shuttle orbiter charging. J. Spacecraft and Rockets 20, 22-25.

Laframboise, J.G. (1983a) Is there a good way to model spacecraft charging in the presence of space-charge coupling, flow, and magnetic field? In: Proc. Air Force Geophys. Lab. Workshop on Natural Charging of Large Space Structures in Near Earth Polar Orbit, edited by R.C. Sagalyn, D.E. Donatelli, and I. Michael, Report No. AFGL-TR-83-0046/Environmental Research Paper No. 825, Air Force Geophysics Laboratory, Massachusetts, pp.57-78. ADA134894

Laframboise, J.G. (1983b) Incident velocity distributions on sampling electrodes of spacecraft plasma instruments. In: Proc. 17th ESLAB Symposium on "Spacecraft/Plasma Interactions and their Influence on Field and Particle Measurements, Report No. ESA SP-198, European Space Agency Scientific and Technical Publications Branch, ESTEC, Noordwijk, The Netherlands, pp.101-108.

Laframboise, J.G. (1985) Calculation of secondary-electron escape currents from inclined spacecraft surfaces in a magnetic field. In: Spacecraft Environmental Interactions Technology 1983, edited by C.K. Purvis and C.P. Pike, NASA Conference Publication 2359/Report No. AFGL-TR-85-0018, Air Force Geophysics Laboratory, Massachusetts, pp. 277-286.

Laframboise, J.G., Kamitsuma, M., and Godard, R. (1982) Multiple floating potentials, "threshold-temperature" effects, and "barrier" effects in high-voltage charging of exposed surfaces on spacecraft. In: Proc. Internat. Symp. on Spacecraft Materials in Space Environment, June 1982, Toulouse, France, European Space Agency, Paris, Publication No. ESA SP-178, pp. 269-275.

Laframboise, J.G., Kamitsuma, M., Prokopenko, S.M.L., Chang, Jen-Shih, and Godard, R. (1982) Numerical simulation of spacecraft charging phenomena at high altitude, Final Report on Grant AFOSR-76-2962, York University.

Laframboise, J.G., Kamitsuma, M. (1983) The threshold temperature effect in high-voltage spacecraft charging. In: Proc. Air Force Geophys. Lab. Workshop on Natural Charging of Large Space Structures in Near Earth Polar Orbit, edited by R.C. Sagalyn, D.E. Donatelli, and I. Michael, Report No. AFGL-TR-83-0046/Environmental Research Paper No. 825, Air Force Geophysics Laboratory, Massachusetts, pp. 293-308. ADA134894

Langmuir, I., and Blodgett, K.B. (1924) Currents limited by space charge between concentric spheres. Phys. Rev. 23, 49.

Parks, D.E., and Katz, I. (1981) Charging of a large object in low polar Earth orbit. In: Spacecraft Charging Technology 1980, NASA Conference Publication 2182/Report No. AFGL-TR-81-0270, Air Force Geophysics Laboratory, Massachusetts, pp. 979-989. ADA114426

Parks, D.E., and Katz, I. (1983a) Electric field effects on ion currents in satellite wakes. In: Spacecraft Environmental Interactions Technology 1983, edited by C.K. Purvis and C.P. Pike, NASA Conference Publication 2359/Report No. AFGL-TR-85-0018, Air Force Geophysics Laboratory, Massachusetts, pp. 195-204.

Parks, D.E., and Katz, I. (1983b) Mechanisms that limit potentials on ionospheric satellites. J. Geophys. Res. 88, 9155-9162.

Parker, L.W. (1970) Theory of the external sheath structure and ion collection characteristics of a rocket-borne mass spectrometer, Report No. AFCRL-71-0105, Air Force Geophysics Laboratory, Hanscom AFB, Massachusetts, U.S.A. AD720833

Parker, L.W., and Whipple, E.C. Jr. (1970) Theory of spacecraft sheath structure, potential, and velocity effects on ion measurements by traps and mass spectrometers, J. Geophys. Res., 75, 4720-4733.

Parrot, M.J.M., Storey, L.R.O., Parker, L.W., and Laframboise, J.G. (1982) Theory of cylindrical and spherical Langmuir probes in the limit of vanishing Debye number. Physics of Fluids 25, 2388-2400.

Singh, N., and Baugher, C.R. (1981), Sheath effects on current collection by particle detectors with narrow acceptance angles. Space Sci. Instrum 5, 295-305.

Whipple, E.C., Warnock, J.M. and Winkler, R.H. (1974), Effects of satellite potential on direct ion density measurements through the plasmapause. J. Geophys. Res. 79, 179-186.

THETA EPS	15.00	30.00	45.00	60.00	75.00	80.00	85.00	89.00
0.00	.965	.865	.707	.500	.258	.174	.087	.017
.20	.991	.931	.796	.585	.311	.209	.105	.020
.50	.999	.978	.892	.704	.397	.271	.137	.027
1.00	.999	.997	.971	.857	.545	.384	.198	.039
2.00	.999	1.000	.999	.982	.802	.617	.342	.070
5.00	.999	1.000	1.000	1.000	.998	.968	.723	.172
10.00	.999	1.000	1.000	.999	1.000	1.000	.971	.338
20.00	.999	1.000	1.000	.999	1.000	1.000	1.000	.617

TABLE 1

Values of the ratio $i = I/I_0$ of escaping to emitted flux, for various values of θ, the angle (in degrees) between the surface normal and the magnetic-field direction, and ϵ, the nondimensional repelling electric field strength. These two quantities appear in the table as THETA and EPS, respectively. These results are accurate to within about 0.5% or better; thus the differences between .999 and 1.000 in the Table are not significant. For $\theta = 0^0$, $i = 1$ for all values of ϵ.

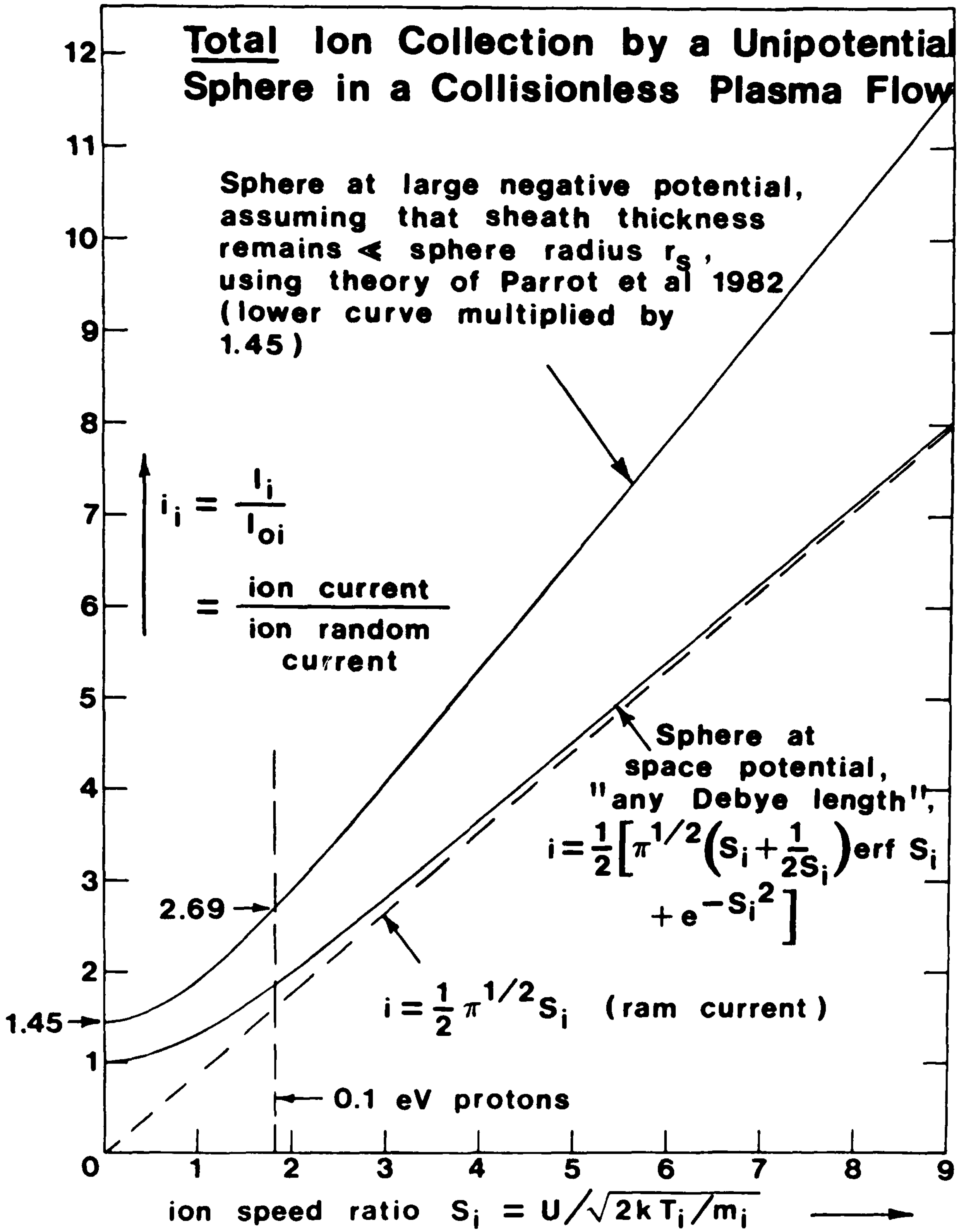

Figure 2.1 Dependence of ion current to a sphere on ion speed ratio.

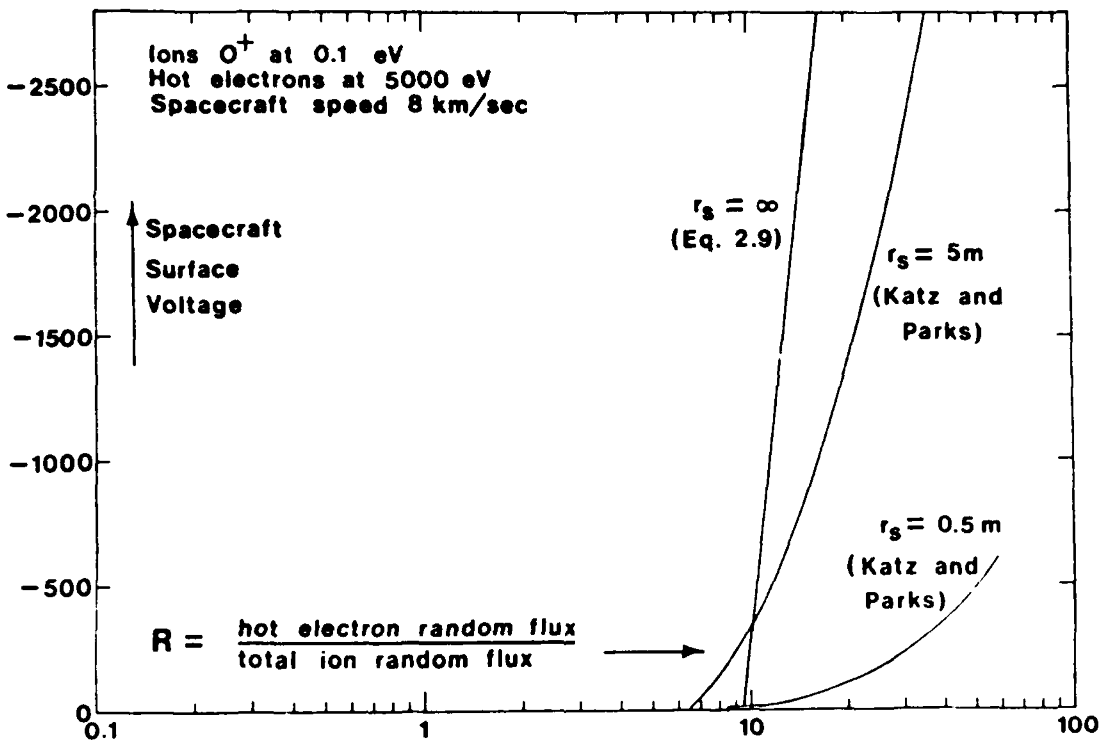

Figure 2.2 Dependence of spacecraft surface potential on hot electron/total ion ambient flux ratio.

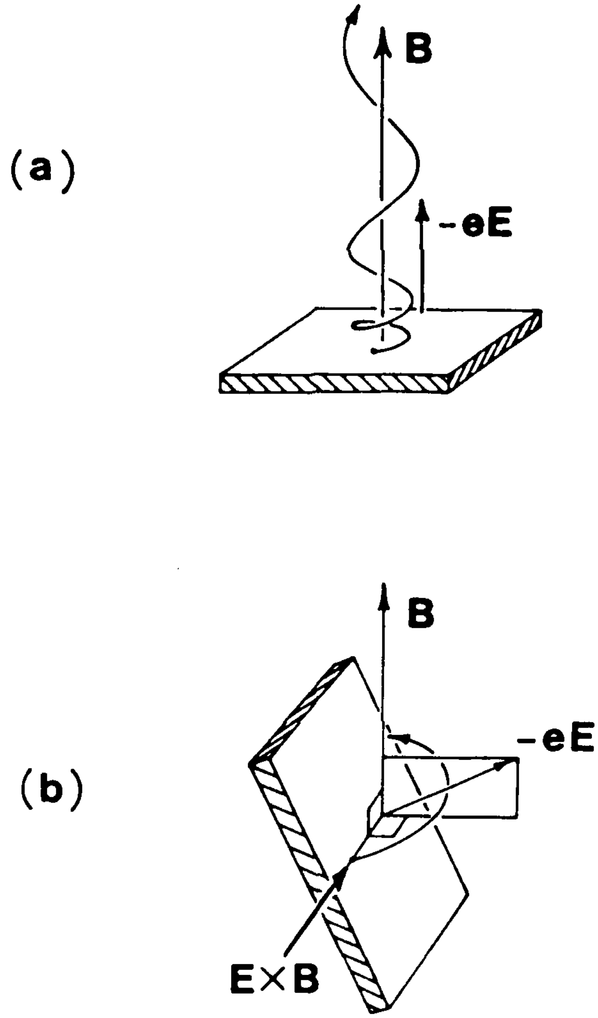

Figure 3.1 Effect of surface orientation on escape of emitted electrons. In (a), the spacecraft surface is perpendicular to the magnetic field $\vec{B}$, and the emitted electrons, which experience an electric force $-e\vec{E}$ directed away from the surface, all escape. In (b), the spacecraft surface is nearly parallel to $\vec{B}$, and almost all of the emitted electrons return to the surface, even though they still experience an electric force directed away from it. Note that the component of $\vec{E}$ perpendicular to $\vec{B}$ results only in an $\vec{E} \times \vec{B}$ drift parallel to the surface.

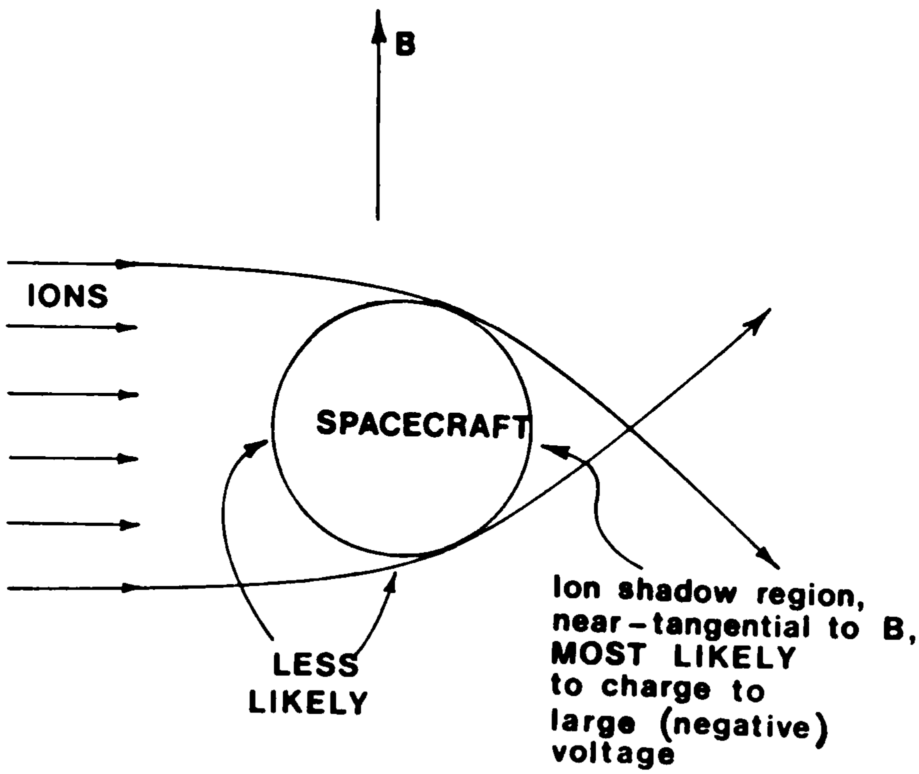

Figure 3.2. Spacecraft simultaneously in a collisionless ion flow and a magnetic field $\vec{B}$.

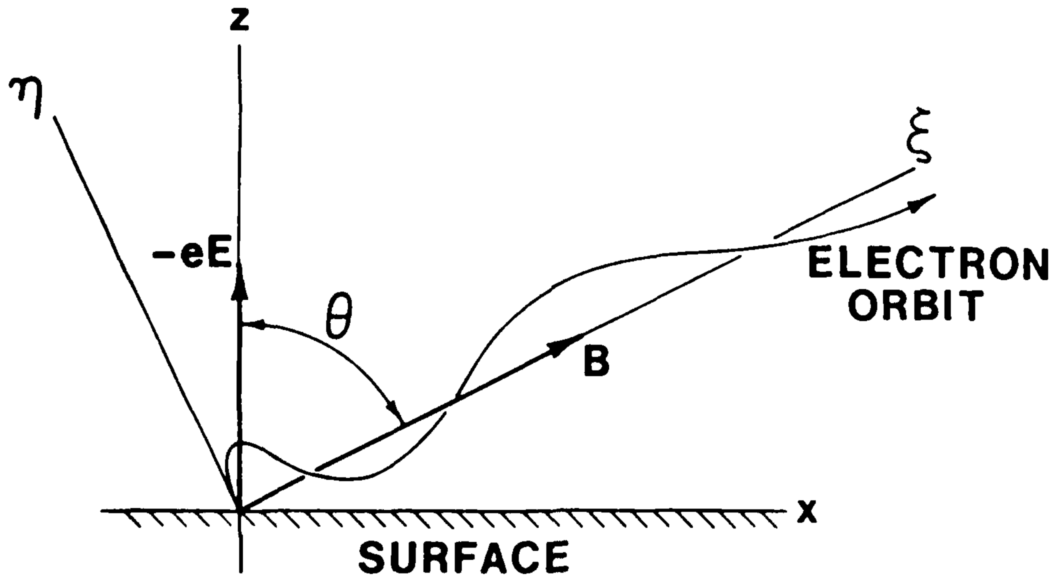

Figure 3.3. Coordinate system for calculating electron escape fluxes. The y-coordinate (not shown) is directed into the plane of the Figure.

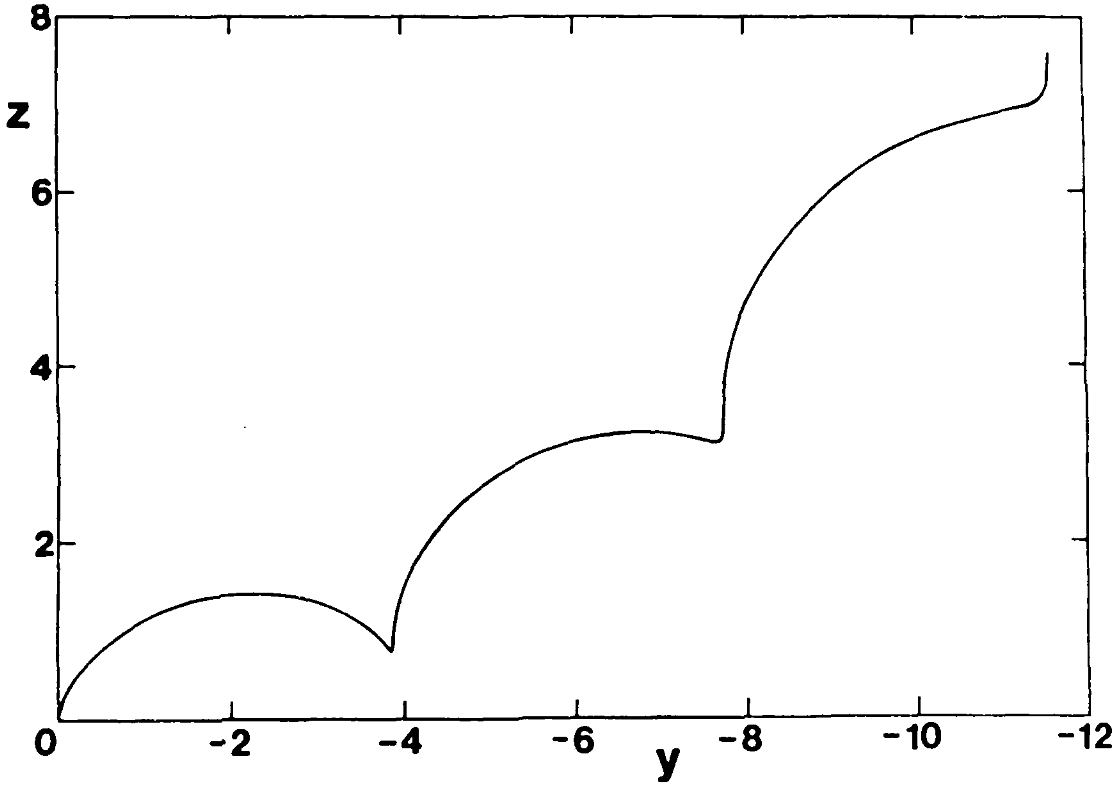

Figure 3.4. Example of an electron orbit having zero initial velocity. The magnetic field $\vec{B}$ is parallel to the (x,z) plane, and makes an angle $\theta = 75^0$ with the z axis. $\epsilon = 1$. Three gyroperiods of the orbit $(0 \leq \tau \leq 6\pi)$ are shown.

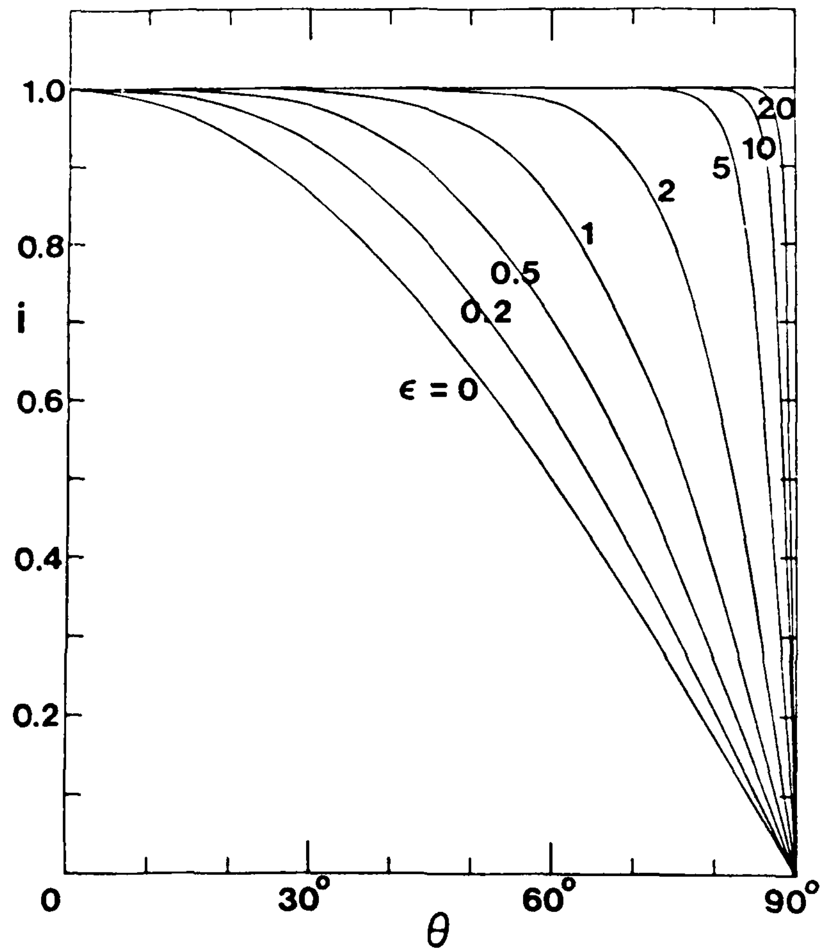

Figure 3.5. Ratio $i = I/I_0$ of escaping to emitted secondary-electron flux, as a function of the angle θ between the surface normal and the magnetic field direction, for various values of the repelling electric field strength parameter $\epsilon = (E/B)(\pi m/2kT)^{\frac{1}{2}}$. The result for $\epsilon = 0$ is given by $i = \cos \theta$.

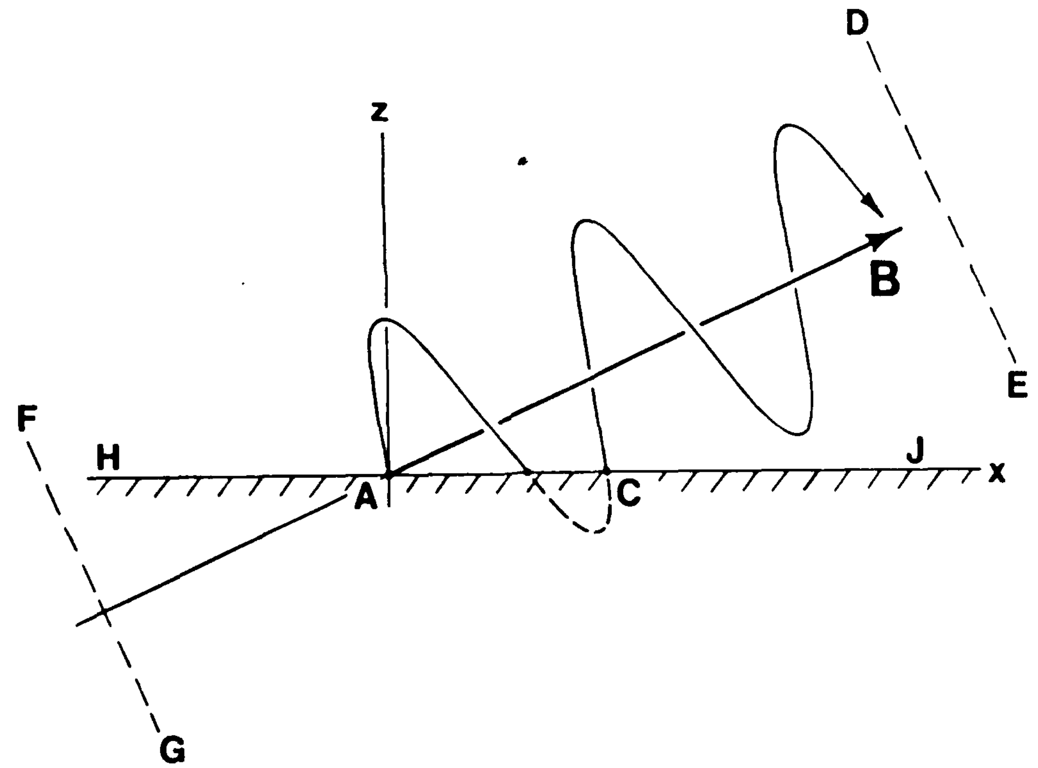

Figure 3.6. Electron orbit for $\epsilon = 0$, fictitiously extended so as to pass through the surface and re-emerge from it.

APPENDIX: LISTING OF COMPUTER PROGRAM USED IN SEC. 3.

Note: In its present form, this program incorrectly predicts nonzero electron escape when $(E_x/E_z)(B_x/B_z) < -1$, i.e. when $e\vec{E}$ has an outward normal component, but its projection along $\vec{B}$ has an inward normal component.

```
FTN4
      PROGRAM SCAPE
C
C     THIS PROGRAM CALCULATES THE ESCAPING FLUX (NORMALIZED BY RANDOM
C     FLUX) OF MAXWELLIAN ELECTRONS EMITTED FROM A PLANE SURFACE IN
C     THE PRESENCE OF UNIFORM ELECTRIC AND MAGNETIC FIELDS. THE
C     SURFACE IS IN THE (X,Y) PLANE.
C
C      DATE IS A 10-CHARACTER USER-SUPPLIED DATE FIELD.
C      NKSES IS THE NUMBER OF CASES TO BE CALCULATED.
C      NDBUG IS A PARAMETER GOVERNING EXTRA OUTPUT FOR DEBUGGING
C     PURPOSES. IF NDBUG > 0,EXTRA OUTPUT OCCURS. IF NDBUG > 1,NDBUG
C     RATHER THAN ONE ELECTRON ORBITS ARE FOLLOWED.
C      NALFA,NPSI, AND NTH ARE THE NUMBERS OF VALUES OF ALPHA, PSI AND
C     THETA (IN DEGREES) TO BE READ IN.
C      NEPS IS THE NUMBER OF VALUES OF EPS TO BE READ IN.
C      NTAU IS NUMBER OF (DIMENSIONLESS) TIME INTERVALS PER ELECTRON
C     GYROPERIOD.
C      MINT SELECTS METHOD OF INTEGRATION.
C     THE ANGLES ALPHA AND PSI DEFINE DIRECTION OF THE ELECTRIC FIELD
C     VECTOR E.
C      ALPHA IS THE ANGLE BETWEEN THE -E DIRECTION AND THE
C     SURFACE NORMAL (THE Z AXIS).
C      PSI IS THE ANGLE BETWEEN THE PLANE
C     CONTAINING THE Z AXIS AND THE -E VECTOR, AND THE (X,Z) PLANE.
C      THETA IS THE ANGLE BETWEEN THE MAGNETIC FIELD VECTOR, WHICH IS
C     ASSUMED TO BE IN THE (X,Z) PLANE, AND THE SURFACE NORMAL.
C      EPS IS DIMENSIONLESS ELECTRIC FIELD STRENGTH, DEFINED AS THE
C     POTENTIAL DIFFERENCE ACROSS A MEAN EMITTED-ELECTRON GYRORADIUS,
C     DIVIDED BY THE EMITTED-ELECTRON TEMPERATURE IN VOLTS.
C      DVX,DVY,AND DVZ ARE STEPSIZES FOR INTEGRATION OVER DIMENSIONLESS
C     VELOCITY. ***WARNING***:THE RESULTING VALUE OF NVZ MUST BE NO
C     LARGER THAN THE DIMENSIONS OF VZ,KNEGZ,KMIN,KESC,ZMIN,AND VZLIM.
C
      DIMENSION VZ(100),KNEGZ(100),KMIN(100),KESC(100),ZMIN(100),
     1VZLIM(100)
      DIMENSION X(361),Y(361),SPARL(361),SPERP(361)
      DIMENSION QSIV(361),ETAV(361),STOR(361)
      DIMENSION TAU(361),CSTAU(361),SNTAU(361),Z(361),DZ(361)
      DIMENSION FLUX(181)
      DIMENSION DATE(5)
      DIMENSION ALPHA(91),PSI(181),THETA(181),EPS(40)
      DIMENSION ITIME(5)
C
      PI=3.14159265
      RTPI=SQRT(PI)
      TOPI=2.0/PI
      TORP=2.0/RTPI
      READ(7,10)DATE,NKSES,NDBUG
   10 FORMAT(5A2,3I5)
      DO 1000 KASE=1,NKSES
C
C     READ SYSTEM CLOCK.
C
   12 ICODE=11
      CALL EXEC(ICODE,ITIME)
      FCENS=ITIME(1)
      FSEC=ITIME(2)
      FMIN=ITIME(3)
      FHR=ITIME(4)
      FDAY=ITIME(5)
C
      IF(NDBUG.GT.0)READ(7,120)BALPH,BPSI,BTHTA,BEPS,BVXIN,BVYIN,BVZIN
```

```
      READ(7,110)NALFA,NPSI,NTH,NEPS,NTAU,MINT
  110 FORMAT(6I5)
      READ(7,120)(ALPHA(I),I=1,NALFA)
      READ(7,120)(PSI(I),I=1,NPSI)
      READ(7,120)(THETA(I),I=1,NTH)
      READ(7,120)(EPS(I),I=1,NEPS)
      READ(7,120)DVX,DVY,DVZ
  120 FORMAT(7E10.3)
C
C     IESC=12 GIVES FORM FEED ON H-P PRINTER.
C
      IESC=12
      WRITE(6,125)IESC,DATE,KASE
  125 FORMAT(A2,1X"FLUX OF SECONDARY ELECTRONS ESCAPING FROM A SURFACE I
     1N UNIFORM E AND B FIELDS. ",5A2," , CASE"I3)
      WRITE(6,130)NALFA,NPSI,NTH,NEPS,NTAU,MINT,DVX,DVY,DVZ
  130 FORMAT(/" NALFA NPSI  NTH NEPS NTAU MINT",7X"DVX",7X"DVY",7X"DVZ"
     1 /1X6I5,1P3E10.3)
      WRITE(6,140)(ALPHA(I),I=1,NALFA)
      WRITE(6,141)(PSI(I),I=1,NPSI)
      WRITE(6,142)(THETA(I),I=1,NTH)
      WRITE(6,143)(EPS(I),I=1,NEPS)
  140 FORMAT(/" ALPHA",1P12E10.3)
  141 FORMAT(/"   PSI",1P12E10.3)
  142 FORMAT(/" THETA",1P12E10.3)
  143 FORMAT(/"   EPS",1P12E10.3)
      KPBUG=0
      KWEER=0
      NVX=INT(9.0/DVX)+1
      NVY=INT(9.0/DVY)+1
      NVZ=INT(4.5/DVZ)+1
      DTAU=2.0*PI/NTAU
      IF(NDBUG.GE.2)NTAU=NDBUG*NTAU
      NTAUP=NTAU+1
      DO 160 ITAU=2,NTAUP
      TAU(ITAU)=DTAU*(ITAU-1)
      CSTAU(ITAU)=COS(TAU(ITAU))
  160 SNTAU(ITAU)=SIN(TAU(ITAU))
      DO 161 IVZ=1,NVZ
  161 VZ(IVZ)=DVZ*(IVZ-1)
C
      DO 900 IALFA=1,NALFA
      ALFA=ALPHA(IALFA)*PI/180.0
      DO 900 IPSI=1,NPSI
      PSII=PSI(IPSI)*PI/180.0
      COPSI=COS(PSII)
      SIPSI=SIN(PSII)
      WRITE(6,166)ALPHA(IALFA),PSI(IPSI)
  166 FORMAT(//1X"ANGLES DEFINING ELECTRIC FIELD DIRECTION: ALPHA = ",
     A 1PE10.3," DEGREES, PSI = "1PE10.3," DEGREES")
      DO 800 IEPS=1,NEPS
      EPSS=EPS(IEPS)
      EX=-EPSS*SIN(ALFA)*COPSI
      EY=-EPSS*SIN(ALFA)*SIPSI
      EZ=-EPSS*COS(ALFA)
      DO 700 ITH=1,NTH
      FETA=THETA(ITH)*PI/180.0
      COSTH=COS(FETA)
      SINTH=SIN(FETA)
      EQSI=EX*SINTH+EZ*COSTH
      EETA=-EX*COSTH+EZ*SINTH
      COA=-EQSI/PI
      COE=TOPI*EY
      COF=TOPI*EETA
C
      SUM=0.0
```

```
      DO 600 IVX=1,NVX
      VXIN=-4.5+DVX*(IVX-1)
      VXINS=VXIN*SINTH
      VXINC=VXIN*COSTH
      DO 600 IVY=1,NVY
      VYIN=-4.5+DVY*(IVY-1)
      DO 500 IVZ=1,NVZ
      VZIN=VZ(IVZ)
      VQSIN=VXINS+VZIN*COSTH
      VETIN=-VXINC+VZIN*SINTH
      COB=VQSIN*TORP
      COC=TORP*VETIN+TOPI*EY
      COD=TORP*VYIN-TOPI*EETA
      ZMIN(IVZ)=-0.0
      KNEGZ(IVZ)=0
      KMIN(IVZ)=0
      X(1)=0.0
      Y(1)=0.0
      SPARL(1)=0.0
      SPERP(1)=0.0
      Z(1)=0.0
      DQSI=COB
      DETA=COC-COE
      DZ(1)=DQSI*COSTH+DETA*SINTH
      D2ZIN=2.0*COA*COSTH+COD*SINTH
      IF(VZIN.EQ.0.0.AND.D2ZIN.LT.0.0)KNEGZ(IVZ)=2
C
C     SEARCH ALONG AN ORBIT FOR A LOCAL MINIMUM IN Z.
C
      IF(MINT.GT.0)GO TO 360
      COG=2.0*COA*COSTH
      COH=COB*COSTH-COE*SINTH
      COI=COC*SINTH
      COJ=COD*SINTH
      DO 350 ITAU=2,NTAUP
      QSI=(COA*TAU(ITAU)+COB)*TAU(ITAU)
      ETA=COC*SNTAU(ITAU)+COD*(1.0-CSTAU(ITAU))-COE*TAU(ITAU)
      X(ITAU)=QSI*SINTH-ETA*COSTH
      Y(ITAU)=COD*SNTAU(ITAU)+COC*(CSTAU(ITAU)-1.0)+COF*TAU(ITAU)
      SPARL(ITAU)=X(ITAU)*COPSI+Y(ITAU)*SIPSI
      SPERP(ITAU)=-X(ITAU)*SIPSI+Y(ITAU)*COPSI
      Z(ITAU)=QSI*COSTH+ETA*SINTH
  350 DZ(ITAU)=COG*TAU(ITAU)+COH+COI*CSTAU(ITAU)+COJ*SNTAU(ITAU)
      GO TO 380
C
C     THE NEXT 25 STATEMENTS USE THE H-P "VECTOR INSTRUCTION SET"
C     (ARRAY PROCESSOR) TO REPLACE LOOP 350, JUST ABOVE, IN ORDER
C     TO SPEED EXECUTION.
C
  360 CALL VSMY(COA,TAU(2),1,STOR(2),1,NTAU)
      CALL VSAD(COB,STOR(2),1,STOR(2),1,NTAU)
      CALL VMPY(STOR(2),1,TAU(2),1,QSIV(2),1,NTAU)
C
      CALL VSSB(1.0,CSTAU(2),1,STOR(2),1,NTAU)
      CALL VSMY(COD,STOR(2),1,STOR(2),1,NTAU)
      CALL VPIV(COC,SNTAU(2),1,STOR(2),1,STOR(2),1,NTAU)
      CALL VPIV(-COE,TAU(2),1,STOR(2),1,ETAV(2),1,NTAU)
C
      CALL VSMY(-COSTH,ETAV(2),1,STOR(2),1,NTAU)
      CALL VPIV(SINTH,QSIV(2),1,STOR(2),1,X(2),1,NTAU)
C
      CALL VSAD(-1.0,CSTAU(2),1,STOR(2),1,NTAU)
      CALL VSMY(COC,STOR(2),1,STOR(2),1,NTAU)
      CALL VPIV(COD,SNTAU(2),1,STOR(2),1,STOR(2),1,NTAU)
      CALL VPIV(COF,TAU(2),1,STOR(2),1,Y(2),1,NTAU)
C
```

```
      CALL VSMY(SIPSI,Y(2),1,STOR(2),1,NTAU)
      CALL VPIV(COPSI,X(2),1,STOR(2),1,SPARL(2),1,NTAU)
C
      CALL VSMY(COPSI,Y(2),1,STOR(2),1,NTAU)
      CALL VPIV(-SIPSI,X(2),1,STOR(2),1,SPERP(2),1,NTAU)
C
      CALL VSMY(SINTH,ETAV(2),1,STOR(2),1,NTAU)
      CALL VPIV(COSTH,QSIV(2),1,STOR(2),1,Z(2),1,NTAU)
C
      COG=2.0*COA*COSTH
      CALL VSMY(COG,TAU(2),1,STOR(2),1,NTAU)
      COH=COB*COSTH-COE*SINTH
      CALL VSAD(COH,STOR(2),1,STOR(2),1,NTAU)
      CALL VPIV(COC*SINTH,CSTAU(2),1,STOR(2),1,STOR(2),1,NTAU)
      CALL VPIV(COD*SINTH,SNTAU(2),1,STOR(2),1,DZ(2),1,NTAU)
C
  380 DO 400 ITAU=2,NTAUP
      IF(Z(ITAU).LT.0.0)KNEGZ(IVZ)=MAX0(KNEGZ(IVZ),1)
      IF(DZ(ITAU).GE.0.0.AND.DZ(ITAU-1).LT.0.0)GO TO 443
  400 CONTINUE
      IF(KNEGZ(IVZ).GT.0)GO TO 402
C
C     NO NEGATIVE VALUES OF Z OR MINIMA IN Z HAVE BEEN FOUND.
C
  401 KESC(IVZ)=1
      GO TO 470
C
C     NEGATIVE VALUES OF Z HAVE BEEN FOUND, BUT NO MINIMUM IN Z. PRINT
C     ORBIT FOR EXAMINATION.
C
  402 KESC(IVZ)=0
      IF(KWEER.GE.3)GO TO 470
      WRITE(6,409)
  409 FORMAT(/" ORBIT DETAILS")
      WRITE(6,410)
  410 FORMAT(6X5HALPHA,7X3HPSI,5X5HTHETA,6X4HEPSS,6X4HVXIN,6X4HVYIN,
     A 6X4HVZIN)
      WRITE(6,411)ALPHA(IALFA),PSI(IPSI),THETA(ITH),EPSS,VXIN,VYIN,VZIN
  411 FORMAT(1X1P7E10.3)
      WRITE(6,412)(I,X(I),Y(I),Z(I),DZ(I),I=1,NTAUP)
  412 FORMAT(/1X3(5X"I",5X"X(I)",5X"Y(I)",5X"Z(I)",4X"DZ(I)")/
     A (1X3(I6,4F9.3)))
      KWEER=KWEER+1
      GO TO 470
C
C     A MINIMUM IN Z HAS BEEN FOUND. DETERMINE ITS Z VALUE ZMIN(IVZ).
C
  443 KMIN(IVZ)=1
      FRACT=DZ(ITAU-1)/(DZ(ITAU-1)-DZ(ITAU))
      TAMIN=TAU(ITAU-1)+FRACT*DTAU
      QSI=(COA*TAMIN+COB)*TAMIN
      ETA=COC*SIN(TAMIN)+COD*(1.0-COS(TAMIN))-COE*TAMIN
      ZMIN(IVZ)=QSI*COSTH+ETA*SINTH
      IF(ZMIN(IVZ).LT.0.0)KMIN(IVZ)=2
      KESC(IVZ)=0
      IF(ZMIN(IVZ).GE.0.0)KESC(IVZ)=1
C
  470 IF(NDBUG.EQ.0)GO TO 500
      IF(BALPH.NE.ALPHA(IALFA))GO TO 500
      IF(BPSI.NE.PSI(IPSI))GO TO 500
      IF(BTHTA.NE.THETA(ITH))GO TO 500
      IF(BEPS.NE.EPSS)GO TO 500
      IF(ABS(VXIN-BVXIN).GT.0.0001)GO TO 500
      IF(ABS(VYIN-BVYIN).GT.0.0001)GO TO 500
      IF(ABS(VZIN-BVZIN).GT.0.0001)GO TO 500
      WRITE(6,409)
```

```
      WRITE(6,410)
      WRITE(6,411)ALPHA(IALFA),PSI(IPSI),THETA(ITH),EPSS,VXIN,VYIN,VZIN
      WRITE(6,412)(I,X(I),Y(I),Z(I),DZ(I),I=1,NTAUP)
  500 CONTINUE
C
C     KESC(IVZ)=1 OR 0 DEPENDING ON WHETHER THE IVZ'TH ORBIT DID OR
C     DID NOT ESCAPE. KMIN(IVZ) > 0 OR = 0 DEPENDING ON WHETHER A LOCAL
C     MINIMUM IN Z WAS OR WAS NOT FOUND. KLIM IS THE FOUND NUMBER OF
C     STARTING OR END POINT VALUES VZLIM(1,2,...,KLIM) FOR INTEGRATION
C     IN VZIN (THE INITIAL Z VELOCITY), FOR ESCAPING ORBITS.
C
      KLIM=0
      IF(KESC(1).EQ.0)GO TO 501
      KLIM=1
      VZLIM(1)=0.0
  501 DO 510 IVZ=2,NVZ
      IF(KESC(IVZ).EQ.KESC(IVZ-1))GO TO 510
      KLIM=KLIM+1
      IF(KMIN(IVZ-1).EQ.0.OR.KMIN(IVZ).EQ.0)GO TO 505
      VZLIM(KLIM)=VZ(IVZ-1)+ZMIN(IVZ-1)/(ZMIN(IVZ-1)-ZMIN(IVZ))*
     A (VZ(IVZ)-VZ(IVZ-1))
      GO TO 510
C
C     AN INTERVAL IN VZIN HAS BEEN FOUND CONTAINING A CHANGE BETWEEN
C     ESCAPE AND NO ESCAPE, BUT A LOCAL MINIMUM IN Z IS NOT FOUND
C     FOR ONE OR BOTH ENDS OF THIS INTERVAL. PRINT ORBIT PARAMETERS FOR
C     EXAMINATION.
C
  505 VZLIM(KLIM)=0.5*(VZ(IVZ-1)+VZ(IVZ))
      KPBUG=KPBUG+1
      IF(KPBUG.GE.6.OR.NDBUG.EQ.0)GO TO 510
      WRITE(6,409)
      WRITE(6,410)
      WRITE(6,411)ALPHA(IALFA),PSI(IPSI),THETA(ITH),EPSS,VXIN,
     1 VYIN,VZ(IVZ)
C
  510 CONTINUE
C
      SIGN=1.0
      VZSUM=0.0
      IF(KLIM.EQ.0)GO TO 530
      DO 520 ILIM=1,KLIM
      VZL=VZLIM(ILIM)
      VZSUM=VZSUM+SIGN*EXP(-VZL*VZL)
  520 SIGN=-SIGN
C
  530 IF(NDBUG.EQ.0)GO TO 600
      IF(BALPH.NE.ALPHA(IALFA).OR.BPSI.NE.PSI(IPSI))GO TO 600
      IF(BTHTA.NE.THETA(ITH).OR.BEPS.NE.EPSS)GO TO 600
      IF(ABS(VXIN-BVXIN).GT..0001.OR.ABS(VYIN-BVYIN).GT..0001)GO TO 600
      WRITE(6,540)(I,KESC(I),KMIN(I),ZMIN(I),I=1,NVZ)
  540 FORMAT(/1X4("     I KESC(I) KMIN(I)    ZMIN(I)")/
     A (1X4(I5,2I8,1P310.3)))
      IF(KLIM.GT.0)WRITE(6,550)(VZLIM(I),I=1,KLIM)
  550 FORMAT(/(" VZLIM  "1P12E10.3))
      WRITE(6,560)VZSUM
  560 FORMAT(/" VZSUM = "1PE10.3)
C
  600 SUM=SUM+VZSUM*EXP(-VXIN*VXIN-VYIN*VYIN)
C
  700 FLUX(ITH)=SUM*DVX*DVY/PI
      IF(IEPS.GT.1)GO TO 771
      WRITE(6,768)(THETA(ITH),ITH=1,NTH)
  768 FORMAT(/9X"THETA",14F8.4/(20X14F8.4))
      WRITE(6,770)
  770 FORMAT("       EPS   "/)
```

```
  771 WRITE(6,772)EPSS,(FLUX(ITH),ITH=1,NTH)
  772 FORMAT(1X1PE10.3,3X0P14F8.5/(20X0P14F8.5))
C
  800 CONTINUE
  900 CONTINUE
C
C      READ SYSTEM CLOCK AGAIN AND PRINT ELAPSED TIME.
C
       CALL EXEC(ICODE,ITIME)
       FC2=ITIME(1)
       FS2=ITIME(2)
       FM2=ITIME(3)
       FH2=ITIME(4)
       FD2=ITIME(5)
       TIMIN=(24.0*(FD2-FDAY)+FH2-FHR)*60.0+FM2-FMIN+(FS2-FSEC+0.01*(FC2-
      A FCENS))/60.0
       WRITE(6,910)KPBUG,TIMIN
  910 FORMAT(/63XI5," INTEGRATION LIMIT FIXUPS. EXECUTION TIME ",F8.2,
      A " MINUTES.")
 1000 CONTINUE
       END
       END$
```

END
DTIC
5-86